

# REVEALING THE INTERACTION BETWEEN THE X-RAY GAS OF STARBURST GALAXY UGC 6697 AND THE HOT INTRACLUSTER MEDIUM OF A1367

M. SUN & A. VIKHLININ

Harvard-Smithsonian Center for Astrophysics, 60 Garden St., Cambridge, MA 02138;

msun@cfa.harvard.edu

Draft version June 29, 2018

## ABSTRACT

We present the result from a *Chandra* observation of an X-ray luminous starburst galaxy UGC 6697, which is embedded in the northwest hot region of A1367 (5 - 6 keV). A very sharp X-ray edge ( $\sim 13$  times of surface brightness jump) at the southeast and a long tail (at least 60 kpc from the nucleus) at the northwest of the galaxy are detected, as expected if the galaxy is moving to the southeast. The X-ray edge, at the midway of the nucleus and the southeast optical disk edge, is also at the same position where the  $H\alpha$  emission is truncated and a radio sharp edge is observed. The X-ray diffuse emission is also enhanced at the southeast, implying ram pressure compression. No extraplanar X-ray component is detected, probably due to the combining effects of weaker outflow activity than that in nuclear starbursts, and external confinement plus stripping. The diffuse thermal gas in UGC 6697 has a temperature of  $\sim 0.7$  keV and a low iron abundance ( $\sim 0.1 - 0.2$  solar). An X-ray point source ( $L_{0.5-10\text{keV}} \sim 2.8 \times 10^{40}$  ergs  $\text{s}^{-1}$ ) is detected on the nucleus, but not highly absorbed. Three off-center ultraluminous X-ray sources, all with  $L_{0.5-10\text{keV}} > 10^{40}$  ergs  $\text{s}^{-1}$ , are also detected. Based on the multi-wavelength data available, we favor that the interaction between the interstellar medium (ISM) and the ICM plays a major role to trigger the starburst in UGC 6697.

*Subject headings:* galaxies: clusters: general — galaxies: clusters: individual (A1367) — X-rays: galaxies — galaxies: individual (UGC 6697) — galaxies: starburst

## 1. INTRODUCTION

The dynamical and thermal properties of the hot intracluster medium (ICM) have long been proposed to play vital roles in shaping the properties of cluster galaxies. One significant question is the effect of the ICM on the cluster star formation rate (SFR). After the discovery of the “Butcher-Oemler effect” in the medium redshift clusters ( $z \approx 0.4$ ; Butcher & Oemler 1978, 1984), it was suggested that compression by the ICM for the first-infall galaxies is the mechanism for star formation in these blue galaxies (e.g., Gunn 1989). Recent 3D simulations on ram pressure stripping of spirals infalling into a cluster (Abadi, Moore & Bower 1999; Quilis, Moore & Bower 2000; Vollmer et al. 2001; Schulz & Struck 2001) have shown the complexity of this process. Star formation is largely suppressed in high density ICM regions due to the depletion of the galactic medium, but SFR can be boosted in less dense ICM regions when the galactic medium is only compressed but not yet stripped. Recently, Bekki & Couch (2003) suggested that strong compression of galactic molecular clouds due to the high pressure of ICM, either static pressure or ram pressure, can trigger starburst activity lasting on the order of  $10^7$  yr. The rich cluster Abell 1367 is a good nearby system to study starburst activity in clusters, where three subgroups containing high fraction of star-formation galaxies are falling into the cluster core (summarized by Cortese et al. 2004). In this work, we present the analysis of the X-ray emission from the most peculiar and the largest galaxy in these infalling groups, UGC 6697, based on our *Chandra* observations.

UGC 6697 is a starburst galaxy with a SFR of  $5 M_{\odot} / \text{yr}$  (Kennicutt, Bothun, & Schommer 1984; Donas et al. 1990) and a high IRAS  $60 \mu\text{m}$  to  $100 \mu\text{m}$  flux ratio ( $f_{60}/f_{100}$ ) of 0.5. The star formation activity is wide spread on the disk and not concentrated on the nucleus (Gavazzi et al. 1995; G95 hereafter). The galaxy lies  $18'$  (or 450 kpc) northwest of the X-ray peak of the rich galaxy cluster A1367 and appears falling into

the cluster. In the optical bands (U, B, V and R; from GOLD Mine, Gavazzi et al. 2003), it is classified as a peculiar galaxy with an asymmetrical appearance. However, its morphology in the H band is rather symmetrical around the nucleus (G95), which implies that the optical asymmetry is mainly caused by the recent star formation in the disk and dust extinction. A radio “trail” on the northwest side was detected by Gavazzi & Jaffe (1987). HI was found to distribute in the similar asymmetrical way as the optical light and radio continuum and 70% of the neutral hydrogen was found in the northwest side of the galaxy (Sullivan et al. 1981; Dickey & Gavazzi 1991). G95 summarized more unusual properties of UGC 6697 based on radio, optical and NIR data: supergiant HII regions, on the periphery of the galaxy, about 10 times more numerous than normal for its luminosity; shocked gas inferred from strong [O I] and [S II] emission; and 10 times more luminous synchrotron radiation than in other similar galaxies. Those peculiarities have been interpreted as due to the dynamical interaction between the ICM and the galaxy gas, assuming UGC 6697 is moving southeast. However, Gavazzi et al. (2001) revealed a complicated velocity field of UGC 6697 and suggested that UGC 6697 is composed of two galaxies interacting.

X-ray emission of the starburst galaxies is a good probe of the mechanical feedback on galactic scales and the ICM-ISM interaction. Fruscione & Gavazzi (1990) first reported X-ray emission from UGC 6697 based on the *Einstein* data. The galaxy was barely resolved in an old *Chandra* observation as it was  $\sim 17'$  from the aim point (Sun & Murray 2002). A new *Chandra* observation centered at  $\sim 1.5'$  east of UGC 6697 has better resolved its X-ray emission as presented in this work.

The average velocity of UGC 6697 is  $6725 \pm 2$  km/s (from NASA/IPAC Extragalactic Database), 245 km/s larger, in the line of sight, than the average velocity of the northwest subcluster of A1367 (from Cortese et al. 2004). In this paper, we adopt the average velocity of the northwest subcluster to

calculate the distance of UGC 6697. Assuming  $H_0 = 70 \text{ km s}^{-1} \text{ Mpc}^{-1}$ ,  $\Omega_M=0.3$ , and  $\Omega_\Lambda=0.7$ , the luminosity distance of UGC 6697 is 94.4 Mpc, and  $1''=0.438 \text{ kpc}$ . The B band luminosity of UGC 6697 ( $L_B$ ) is  $5 \times 10^{10} L_\odot$ . Uncertainties quoted are  $1 \sigma$ .

## 2. *Chandra* OBSERVATIONS

A 48 ksec *Chandra* observation was performed with the Advanced CCD Imaging Spectrometer (ACIS) on January 24, 2003. The data analysis is the same as the one presented in Sun et al. (2004), as the same *Chandra* pointing is analyzed. The calibration files used correspond to CALDB 2.28 from the *Chandra* X-ray Center (CXC).

### 2.1. The X-ray diffuse emission in UGC 6697

The *Chandra* count image of UGC 6697 is shown in Fig. 1. The X-ray emission is enhanced in the southeast part of the galaxy with a sharp edge at the southeast end. A diffuse tail is observed to the northwest of the galaxy. We measured the *Chandra* surface brightness (exposure-corrected) along two slices to trace the tail and the edge (Fig. 1). A brightness jump of  $\sim 13$  times is observed across the edge. The width of the edge is less than  $1.5''$  (or  $0.7 \text{ kpc}$ ). The tail extends all the way to the edge of the S3 chip (or at least  $60 \text{ kpc}$  from the nucleus). These features imply the action of ram pressure as the galaxy is moving to the southeast. The X-ray emission of UGC 6697 appears constrained to the plane with no extraplanar component generally found in starburst galaxies in the field or in poor environments (e.g., Strickland et al. 2004). Since the starburst-driven superwind can have a velocity of  $\lesssim 1000 \text{ km/s}$ , not very smaller than the expected velocity of UGC 6697, the lack of significant extraplanar component implies that the outflows in UGC 6697 are weaker than that of nuclear starburst (e.g., M82) and can be easily stripped away by ram pressure. For its IR luminosity ( $L_{\text{IR}} = 4.3 \times 10^{10} L_\odot$ ), UGC 6697 is among the X-ray brightest starbursts known (Strickland et al. 2004), which is likely due to the compression by ram pressure and static ambient pressure. The X-ray contours, superposed on the B band optical image, are shown in Fig. 2. The X-ray edge is well inside the stellar emission of the galaxy, which is much more symmetric than the X-ray emission since stars are not affected by the ram pressure.

We also compare the diffuse X-ray emission with the  $H\alpha$  emission (Fig. 2). It had long been noticed that the  $H\alpha$  emission truncates interior to the optical continuum emission (G95). Only when the X-ray emission is well resolved, do we notice that the truncation of  $H\alpha$  emission is at the same position as the X-ray edge. Within the galaxy, a positive correlation of  $H\alpha$  and X-ray emission is observed, which implies that the X-ray emitting gas is mainly located in the recent star formation regions.

The integrated spectrum of the diffuse emission (Fig. 3) was studied. Since the system is close to edge-on, the average absorption is likely higher than the Galactic value ( $2.2 \times 10^{20} \text{ cm}^{-2}$ ). The average optical extinction was estimated to be  $\sim 1 \text{ mag}$  by G95, which corresponds to an absorption excess of  $\sim 1.8 \times 10^{21} \text{ cm}^{-2}$  based on the averaged relation (with large dispersion) derived by Predehl & Schmitt (1995). We present the spectral fits both with absorption allowed to vary and with it fixed at the Galactic value (Table 1). Both MEKAL and VMEKAL models were applied. The solar photospheric abundance table by Anders & Grevesse (1989) is adopted.

VMEKAL model gives slightly better fits. The gas temperature is  $\sim 0.7 \text{ keV}$ . The derived absorption is comparable to or not much higher than the Galactic value. This is consistent with the bright near-Ultraviolet (UV) emission from the galaxy (Marcum et al. 2001). The  $0.5 - 10 \text{ keV}$  luminosity is  $1.0 - 1.2 \times 10^{41} \text{ ergs s}^{-1}$ . The iron abundance is low, less than 0.35 solar (90% higher limit) in the VMEKAL fit. Adding one more MEKAL component does not improve the fit significantly. Since the X-ray emission of X-ray binaries is dominated by the several most luminous ones, the unresolved point source contribution is small,  $< 5\%$  based on the spectral analysis. Low metallicity measured from the global spectrum of the starburst galaxy has been reported and discussed before (e.g., Weaver, Heckman & Dahlem 2000). Recent work by Fabbiano et al. (2004) on the Antennae demonstrates that when the data allows spectroscopy in individual regions to better disentangle the multi-component X-ray gas, solar or over-solar abundances are derived in active star-formation regions, although the global spectrum of Antennae only shows a small abundance. Therefore, the X-ray emitting gas of UGC 6697 is also very likely multi-phase, which makes the estimate of emission measure (or gas density) very uncertain, due to the degeneracy between the abundance and emission measure. Besides the global temperature, we also examined the hardness ratio distribution in UGC 6697 but found no significant difference across the galaxy with the current statistics ( $\sim 810$  counts total in the  $0.7 - 5 \text{ keV}$  band, from the diffuse emission of UGC 6697). Assuming a dimension of  $2.5' \times 2.5' \times 0.4'$  oblate spheroid and a best-fit VMEKAL model (Table 1), the average electron density is  $4.6 \times 10^{-3} f^{-1/2} \text{ cm}^{-3}$  and the total mass of the detected X-ray emitting gas in UGC 6697 is  $3.1 \times 10^9 f^{1/2} M_\odot$ , where  $f$  is the filling factor of the X-ray emitting gas.

The surrounding ICM (projected) has a temperature of  $\sim 7 - 8$  times the X-ray gas in UGC 6697 (Table 1). We argue that UGC 6697 is not in a low density region along the line of sight because the observed sharp X-ray edge indicates a large ram pressure and the northwest subcluster is not very massive (velocity dispersion of  $\sim 770 \text{ km/s}$ , Cortese et al. 2004). The  $\beta$ -model fit to the northwest subcluster by Donnelly et al. (1998) gives an electron density of  $\approx 5.4 \times 10^{-4} \text{ cm}^{-3}$  at the projected position of UGC 6697, and  $> 3.6 \times 10^{-4} \text{ cm}^{-3}$  if the galaxy is within  $10'$  (or  $263 \text{ kpc}$ ) of its projected position along the line of sight. In this work, we take a typical value of  $4.5 \times 10^{-4} \text{ cm}^{-3}$ . The ICM thermal pressure is then  $7.9 \times 10^{-12} \text{ dyn cm}^{-2}$  for an ICM temperature of  $5.7 \text{ keV}$  (Table 1). For comparison, the ram pressure is  $8.7 \times 10^{-12} (v_{\text{gal}} / 1000 \text{ km/s})^2 \text{ dyn cm}^{-2}$ .

### 2.2. X-ray point sources in UGC 6697

Four X-ray point sources (P1 - P4) were detected in UGC 6697 (Fig. 2). Spectral fits were made to the integrated spectrum of four sources (Table 1), which shows that they indeed are hard X-ray sources. Their properties are listed in Table 2. P2 and P3 are a little extended but that extension may come from the nearby diffuse emission as all four sources are hard X-ray sources. We plot the positions of the four sources on the *HST* UV image (Fig. 4). The position of P3 is consistent with the proposed nuclear position of UGC 6697 (the north blue knot A4 in Gavazzi et al. 2001), which is also the peak in the NIR H band and radio emission. No significant absorption excess ( $> 10^{21} \text{ cm}^{-2}$ ) is found to P3. Its  $0.5 - 10 \text{ keV}$  luminosity is  $2.6 - 3.0 \times 10^{40} \text{ ergs s}^{-1}$ . P1, P2 and P4 have  $0.5 - 10 \text{ keV}$  luminosity of  $1.0 - 2.2 \times 10^{40} \text{ ergs s}^{-1}$ . P2 is in a  $H\alpha$  and UV

bright region. P1 is positionally coincident with a knot in the *HST* image, while P4 is  $\sim 0.3$  kpc west to a bright knot. *HST* I-band image is then examined. Both knots are very blue, actually comparable or bluer than the bright complex  $7''$  southeast of P4 (or region c2 in G95). Thus, P1 and P4 may be associated with young star clusters, similar to other Ultraluminous X-ray sources detected in starburst galaxies (e.g., Fabbiano, Zezas & Murray 2001; Kaaret et al. 2004). The summed spectrum of P1, P2 and P4 is consistent with that of high-mass X-ray binary (HMXB) (Table 1). The total 2 - 10 keV luminosity of these three ultraluminous X-ray sources (ULXs) is  $\sim 2.9 \times 10^{40}$  ergs  $s^{-1}$ , which is close to the predicted total X-ray luminosity of HMXBs in UGC 6697 ( $3.3 \times 10^{40}$  ergs  $s^{-1}$ ) based on the  $L_X$  - SFR relation (Grimm, Gilfanov & Sunyaev 2003). This again demonstrates that these ULXs are tightly related to the starburst. Source confusion in UGC 6697 is not expected to affect the number of  $> 10^{40}$  ergs  $s^{-1}$  sources much because: 1) the X-ray emission is dominated by the most luminous sources; 2) the star formation in UGC 6697 is wide spread and not concentrated in the nuclear region; 3) on average, less than one bright X-ray source is expected in or close to a star cluster (e.g., Kaaret et al. 2004). We also performed the K-S test to the X-ray light curves of these point sources but found no significant variations.

### 2.3. X-ray emission from 2MASX J11434983+1958343

Diffuse X-ray emission is also detected from the nearby dwarf spiral galaxy 2MASX J11434983+1958343 to the north of UGC 6697 (Fig. 2 and 4). This dwarf galaxy is  $H\alpha$  bright (Fig. 2) and is only  $\sim 12$  kpc to the plane of UGC 6697 at the projected position. Assuming a massive halo of  $2 \times 10^{12} M_\odot$  within 20 kpc of UGC 6697, the escaping velocity at 20 kpc is 930 km/s, somewhat larger than the velocity difference between the dwarf galaxy and UGC 6697 ( $\sim 800$  km/s). Therefore, the dwarf galaxy is still possible to be bound with UGC 6697. Its X-ray emission is soft and the estimated 0.5 - 10 keV luminosity is  $4 \times 10^{39}$  ergs  $s^{-1}$ . The X-ray emission may come from the gas heated by active star formation (probably triggered by the tidal force of UGC 6697) in the dwarf galaxy.

## 3. DISCUSSION

### 3.1. The stripping of UGC 6697's X-ray emitting gas

This *Chandra* observation presents strong evidence for the interaction between the X-ray gas of UGC 6697 and the surrounding ICM, caused primarily by the motion of UGC 6697 towards the southeast, relative to the surrounding ICM. Although a clear surface brightness edge is found in the X-ray data, the velocity of the galaxy cannot be well constrained from the X-ray data because of the unknown geometry of the galactic X-ray emitting gas and the large uncertainty in the emission measure from the poor determination of abundance. If we simply assume the galaxy is viewed edge-on and the X-ray gas is in a disk with a filling factor of unity, the average electron density at the southeast end is  $1 - 2 \times 10^{-2}$   $cm^{-3}$ , using the emission measured derived from the VMEKAL fit. This yields an internal thermal pressure 2.7 - 5.4 times the ICM thermal pressure. The X-ray ISM density just inside the edge is expected to be smaller than the average value. Thus, the velocity of UGC 6697 through the ICM is  $< 1.2 - 2.0 \times 10^3$  km/s for pressure balance. UGC 6697's direction of motion should be close to its disk plane, which makes the ram pressure stripping very difficult. To the first order, we can apply the simple criterion for ram pressure stripping given in Gunn & Gott (1972).

Even if we assume a small angle of 20 degrees between the disk plane and direction of motion, the critical velocity of UGC 6697 is  $\sim 3000$  km/s (larger for smaller angle) for its X-ray ISM to be stripped out of the plane. Thus, although ram pressure can explain the southeast edge, it is not strong enough in the current environment to fully strip the X-ray gas and other galactic medium. As pointed out by Nulsen (1982), stripping by transport processes may be much more important than ram pressure stripping. The typical mass loss rate due to Kelvin-Helmholtz (K-H) instability is (Nulsen 1982):

$$\begin{aligned} \dot{M}_{KH} &\approx \pi r^2 \rho_{ICM} v_{gal} \\ &= 16.5 \left( \frac{n_{e,ICM}}{4.5 \times 10^{-4} cm^{-3}} \right) \left( \frac{r}{20 kpc} \right)^2 \left( \frac{v_{gal}}{1000 km/s} \right) M_\odot / yr \end{aligned}$$

The X-ray gas mass in the tail is  $\sim 10^8 M_\odot$ , which can be explained by the K-H instability acting for a time duration shorter than or comparable to the lifetime of the starburst ( $\sim 10^7$  yr). The mass loss due to thermal conduction is  $\sim 3.5$  times larger (Nulsen 1982), but the efficiency of thermal conduction is uncertain due to the presence of magnetic fields implied by the strong radio emission. The field lines may have been stretched and entangled at the boundary in the stripping process to largely suppress the thermal conduction, as what was found for the cool coronae in hot clusters (e.g., Sun et al. 2004). Besides being the gas removed by the K-H instability at the front and the sides, the X-ray tail of UGC 6697 may have minor contribution from the gas heated by active star formation in the tail (implied by its blue color and the event of the Type II SN 1986C there). With a similar hardness ratio as the X-ray gas in bright regions, the X-ray tail is not likely to be the concentrated ICM emission by e.g., Bondi accretion, as the ICM temperature is high (5 - 6 keV) and the galaxy velocity is likely large. The current SFR is  $\sim 5 M_\odot yr^{-1}$ , which will likely last for about several  $10^7$  yr. Since massive stars only have lifetimes on the order of  $10^6$  yr, the mass loss rate from stars due to stellar winds and SN explosions is an order of magnitude higher than the SFR and can replenish for the large mass lost due to transport processes and ram pressure stripping.

The southeast edge is very sharp. For the measured gas temperature and density inside and outside of the ICM-ISM boundary, the mean free path of electrons in the hot ICM is  $\sim 22$  kpc. The mean free path of electrons from the hot ICM to the cool ISM is  $\sim 4.3 (n_{e,ISM}/10^{-3} cm^{-3})^{-1}$  kpc, while the mean free path of electrons from the cool ISM to the hot ICM is  $\sim 4.7$  kpc (Spitzer 1962). These values are much larger than the upper limit on the width of the edge ( $\sim 0.7$  kpc). Thus, the particle diffusion across the boundary has to be suppressed by at least 6 times, similar to the situation in cluster cold fronts (Vikhlinin et al. 2001).

The X-ray tail of UGC 6697 is only the second known for a spiral in a rich cluster, next to the galaxy C153 in the 3.2 keV cluster A2125 (Wang et al. 2004). Because of its proximity (compared to A2125 at  $z=0.247$ ), UGC 6697 is the best example known for the stripping of a spiral's X-ray gas in a rich cluster (e.g., no gas temperature measured for the X-ray gas of C153). This phenomenon should be rare in the elliptical-dominated rich clusters, as high star formation activity, which only lasts  $\sim 10^7$  yr, is required to replenish the gas loss by fast stripping. In the case of UGC 6697, the edge-on stripping also makes it easier to retain the galactic X-ray gas.

### 3.2. A starburst triggered by the ICM-ISM interaction?

Although ram pressure is not large enough to deplete the galactic gas (even only the X-ray gas), it can still significantly impact the evolution of UGC 6697. It has been suggested that the starburst in UGC 6697 was triggered by the compression of the hot ICM (e.g. G95). This is an interesting question to address, since the mechanism to cause the starburst activity in UGC 6697 may be related to the Butcher-Oemler effect at the medium redshift. The *Chandra* data clearly show a leading edge produced by the ram pressure at the front. The positional coincidence of the X-ray edge and the  $H\alpha$  truncation position implies their connection. The  $H\alpha$  emission is mainly from  $\sim 10^4$  K gas heated by the nearby young massive stars and is sensitive to stellar population with ages of  $< 10^7$  yr. A definite edge, well inside the optical continuum image, implies the truncation of star formation activity upstream from the edge. This may be best explained by the action of ram pressure, if the starburst activity in this galaxy is triggered by the interaction with the ICM. As Strickland et al. (2000) show for the nearby starburst galaxy NGC 253, the X-ray emission is mainly from the regions where the fast SB-driven wind interacts with the denser ambient ISM. Since the mass loss rate from stars due to wind and SN explosions is high and the starburst duration is short, the X-ray diffuse emission generally traces the star formation regions, as shown by the general correlation between X-ray emission and  $H\alpha$  emission in starburst galaxies. Thus, both the X-ray edge and the  $H\alpha$  edge may reflect the current front of active star formation. Upstream from the front, the galaxy is still bright in U band (G95). Since the UV flux is sensitive to the stellar population of age  $\approx 10^8$  yr, the stellar population upstream from the front is indeed older. Most of ISM there has been stripped so the current star formation activity is weaker. There is also a significant radio edge at the position of the  $H\alpha$  edge (G95). The synchrotron radiation there may be boosted by the compression of magnetic field due to the ram pressure. Thus, the three edges (radio,  $H\alpha$  and X-ray) may all correspond to the same front where the star formation is currently truncated outside due to stripping. The starburst activity at the front and inside the front is triggered by the interaction with the ICM. The properties of UGC 6697's environment match those assumed in the simulation by Bekki & Couch (2003), e.g., ICM density not too high to cause too much stripping. The SFR predicted in their simulation is  $0.1 - 0.6 M_{\odot} \text{ yr}^{-1}$  for  $\sim 10^7$  yr for a single cloud. This can easily explain the total SFR of UGC 6697. UGC 6697 may not be a perfect edge-on galaxy from its  $H\alpha$  emission and the direction of motion of the galaxy may not align exactly with the disk plane of the galaxy. Thus, a velocity component to the north could explain the largely enhanced  $H\alpha$  and radio emission there compared to the south.

However, Gavazzi et al. (2001) proposed that UGC 6697 is composed of two interacting galaxies. The smaller one lies behind the main galaxy and the northwest tail is a tidal tail of

the main galaxy. In this scenario, UGC 6697 is like an Antennae galaxy in a specific configuration viewed edge-on, i.e., two galaxy planes and our line of sight are nearly in the same plane. While the idea is attractive to explain the complex velocity field, there is no features detected in either the *Chandra* image or the hardness ratio map that indicates the interaction of two galaxies. There is also no bright X-ray enhancement around the nucleus (P3), as expected from the nuclear starburst induced by tidal interaction. The H-band image (G95) also looks very normal for single galaxy. Nevertheless, the peculiarities of UGC 6697 cannot be all explained by ram pressure stripping. The warp at the southeast end of the stellar disk is a clear indication of tidal interaction by the companion galaxies (visible in Fig. 2 and Fig. 4), if not by the proposed second galaxy (Gavazzi et al. 2001). To sum up, we consider that the ICM-ISM interaction plays a major effect on the wide-spread star formation in UGC 6697, but tidal effects need to be carefully examined, from the multi-wavelength data and simulations.

## 4. CONCLUSION

In this work, we present clear evidence, a sharp leading edge and a long X-ray tail (at least 60 kpc from the nucleus), for the interaction between the  $\sim 0.7$  keV X-ray gas of the starburst galaxy UGC 6697 and its surrounding hot ICM of A1367 ( $\sim 5.7$  keV) from the *Chandra* observation. This rare case is the best-known example of the X-ray gas of a spiral being stripped by the ICM of a rich cluster and only the second known. The X-ray edge is caused by ram pressure as the galaxy falls through the hot ICM. The X-ray emission of UGC 6697, most likely from the gas heated by SN explosions, appears confined to the plane and no extraplanar component is detected. The derived iron abundance from the global spectrum is low ( $< 0.35$  solar for the 90% higher limit). Apart from an X-ray point source detected from the nucleus, three ULXs ( $L_{0.5-10\text{keV}} > 10^{40}$  ergs  $\text{s}^{-1}$ ) are detected with hard spectra. The estimated total X-ray luminosity of HMXBs and the SFR of UGC 6697 follow the  $L_X$  - SFR relation by Grimm et al. (2003), which implies that these luminous sources are the products of the ongoing starburst. The X-ray edge is at the same position as the  $H\alpha$  edge and the radio edge-like feature. We suggest that these three edges all correspond to the same front. Star formation is truncated outside of the front and the starburst inside of the front is likely triggered by the ICM-ISM interaction.

We thank W. Forman, C. Jones and P. Nulsen for valuable comments. We also thank the referee G. Gavazzi for prompt comments. We are grateful to G. Gavazzi for providing us the optical data of UGC 6697. This research has made use of the GOLD Mine Database, operated by the Universita' degli Studi di Milano-Bicocca. The financial support for this work was provided by *Chandra* grant GO3-4161X.

## REFERENCES

- Abadi, M. G., Moore, B., & Bower, R. G. 1999, *MNRAS*, 308, 947  
 Anders, E., & Grevesse N. 1989, *Geochimica et Cosmochimica Acta*, 53, 197  
 Bekki, K., & Couch, W. J. 2003, *ApJ*, 596, 13L  
 Butcher, H., & Oemler, A. Jr. 1978, *ApJ*, 219, 18  
 Butcher, H., & Oemler, A. Jr. 1984, *ApJ*, 285, 426  
 Cortese, L., Gavazzi, G., Boselli, A., Iglesias-Paramo, J., Carrasco, L. 2004, *A&A*, 425, 429  
 Dickey, J. M., Gavazzi, G. 1991, *ApJ*, 373, 347  
 Donas, J., Buat, V., Milliard, B., & Laget, M. 1990, *A&A*, 235, 60  
 Donnelly, R. H. et al. 1998, *ApJ*, 500, 138  
 Fabbiano, G., Zezas, A., Murray, S. S. 2001, *ApJ*, 554, 1035  
 Fabbiano, G. et al. 2004, *ApJ*, 605, L21  
 Fruscione, A., Gavazzi, G. 1990, *A&A*, 230, 293  
 Gavazzi, G., & Jaffe, W. 1987, *A&A*, 186, L1  
 Gavazzi, G., et al. 1995, *A&A*, 304, 325 (G95)  
 Gavazzi, G. et al. 2001, *A&A*, 377, 745  
 Gavazzi, G., Boselli, A., Donati, A., Franzetti, P., Scodreggio, M. 2003, *A&A*, 400, 451

- Grimm, H. J., Gilfanov, M., Sunyaev, R. 2003, MNRAS, 339, 793  
 Gunn, J. E., & Gott, J. R., III 1972, ApJ, 176, 1  
 Gunn, J. E. 1989, The Epoch of Galaxy Formation, p. 167, eds Frenk, C. S., Kluwer, Dordrecht  
 Kaaret, P., Alonso-Herrero, A., Gallagher, J. S., Fabbiano, G., Zezas, A., Rieke, M. J. 2004, MNRAS, 348, L28  
 Kennicutt, R. C., Bothun, G. D., & Schommer, R. A. 1984, AJ, 89, 1279  
 Marcum, P. M. et al. 2001, ApJS, 132, 129  
 Nulsen, P. E. J. 1982, MNRAS, 198, 1007  
 Predehl, P., Schmitt, J. H. M. M. 1995, A&A, 293, 889  
 Quilis, V., Moore, B., & Bower, R. G. 2000, Science, 288, 1617  
 Schulz, S., & Struck, C. 2001, MNRAS, 328, 185  
 Spitzer, L. 1962, Physics of Fully Ionized Gases (New York: Interscience)  
 Strickland, D. K. et al. 2000, AJ, 120, 2965  
 Strickland, D. K. et al. 2004, ApJ, 606, 829  
 Sullivan, W., Bothun, G., Bates, B., Schommer, R. 1981, AJ, 86, 91  
 Sun, M., Murray, S. S. 2002, ApJ, 576, 708  
 Sun, M., Vikhlinin, A., Forman, W., Jones, C., Murray, S. S. 2004, ApJ, in press (astro-ph/0408425)  
 Vollmer, B., Cayatte, V., Balkowski, C., Duschl, W. J. 2001, ApJ, 561, 708  
 Wang, Q. D., Owen, F., Ledlow, M. 2004, ApJ, 611, 821  
 Weaver, K. A., Heckman, T. M., Dahlem, M. 2000, ApJ, 534, 684  
 Vikhlinin, A., Markevitch, M., Murray, S. S. 2001, ApJ, 551, 160

TABLE 1  
THE SPECTRAL FITS

	Model	Absorption <sup>a</sup>	Parameters <sup>b</sup>	$\chi^2/\text{d.o.f.}$	$L_{0.5-10\text{keV}}^c$	$L_{\text{bol}}^c$
UGC 6697 diffuse emission <sup>d</sup>	MEKAL	(0.22)	$T=0.77^{+0.05}_{-0.06}$ , $Z=0.07^{+0.03}_{-0.02}$	29.4/21	0.93	1.95
		$0.67^{+0.70}_{-0.33}$	$T=0.66^{+0.11}_{-0.06}$ , $Z=0.05^{+0.02}_{-0.01}$	28.6/20	1.24	2.52
	VMEKAL	(0.22)	$T=0.80^{+0.06}_{-0.10}$ , $O=1.1^{+0.7}_{-0.5}$ , $Si=0.2^{+0.4}_{-0.2}$ , $Fe=0.17^{+0.09}_{-0.06}$	23.3/17	0.96	1.63
		$0.69^{+0.73}_{-0.49}$	$T=0.74^{+0.09}_{-0.16}$ , $O=1.0^{+0.9}_{-0.61}$ , $Si=0.2^{+0.3}_{-0.2}$ , $Fe=0.12^{+0.08}_{-0.03}$	22.3/16	1.26	2.28
Surrounding ICM <sup>e</sup>	MEKAL	(0.22)	$T=5.66^{+0.70}_{-0.55}$ , $Z=0.04^{+0.18}_{-0.04}$	100.8/90	-	-
Four point sources <sup>f</sup>	Power law	(0.22)	$\Gamma=1.60^{+0.10}_{-0.09}$	16.0/24	0.77	2.73
		$0.82^{+0.66}_{-0.50}$	$\Gamma=1.77^{+0.22}_{-0.16}$	14.5/23	0.77	2.34
	Bremsstrahlung	(0.22)	$T=6.7^{+2.7}_{-1.7}$	14.9/24	0.68	0.95
		$0.24^{+0.66}_{-0.50}$	$T=6.6^{+3.9}_{-2.1}$	14.9/23	0.68	0.95
Three point sources <sup>g</sup>	Power law	(0.22)	$\Gamma=1.68\pm 0.15$	26.7/24	0.47	1.41
		$1.65^{+0.93}_{-0.76}$	$\Gamma=1.98^{+0.27}_{-0.19}$	23.3/23	0.50	1.51
	Bremsstrahlung	(0.22)	$T=6.5^{+3.7}_{-1.9}$	24.9/24	0.42	0.56
		$0.76^{+0.69}_{-0.54}$	$T=4.7^{+2.8}_{-1.5}$	24.0/23	0.41	0.56

<sup>a</sup> The absorption column, fixed (in brackets, the Galactic value) or free, is in unit of  $10^{21} \text{ cm}^{-2}$ .

<sup>b</sup> The temperature unit is keV and abundances are in solar abundances.

<sup>c</sup> The unit of X-ray luminosity is  $10^{41} \text{ ergs s}^{-1}$ .

<sup>d</sup> Diffuse emission from the elliptical region in Fig. 1

<sup>e</sup> Cluster diffuse emission within  $3' \times 2'$  (semimajor axis  $\times$  semiminor axis) ellipse centered on UGC 6697 (sources excluded)

<sup>f</sup> Sum spectrum of four X-ray point sources in UGC 6697

<sup>g</sup> Sum spectrum of three X-ray point sources (excluding the nucleus source P3)

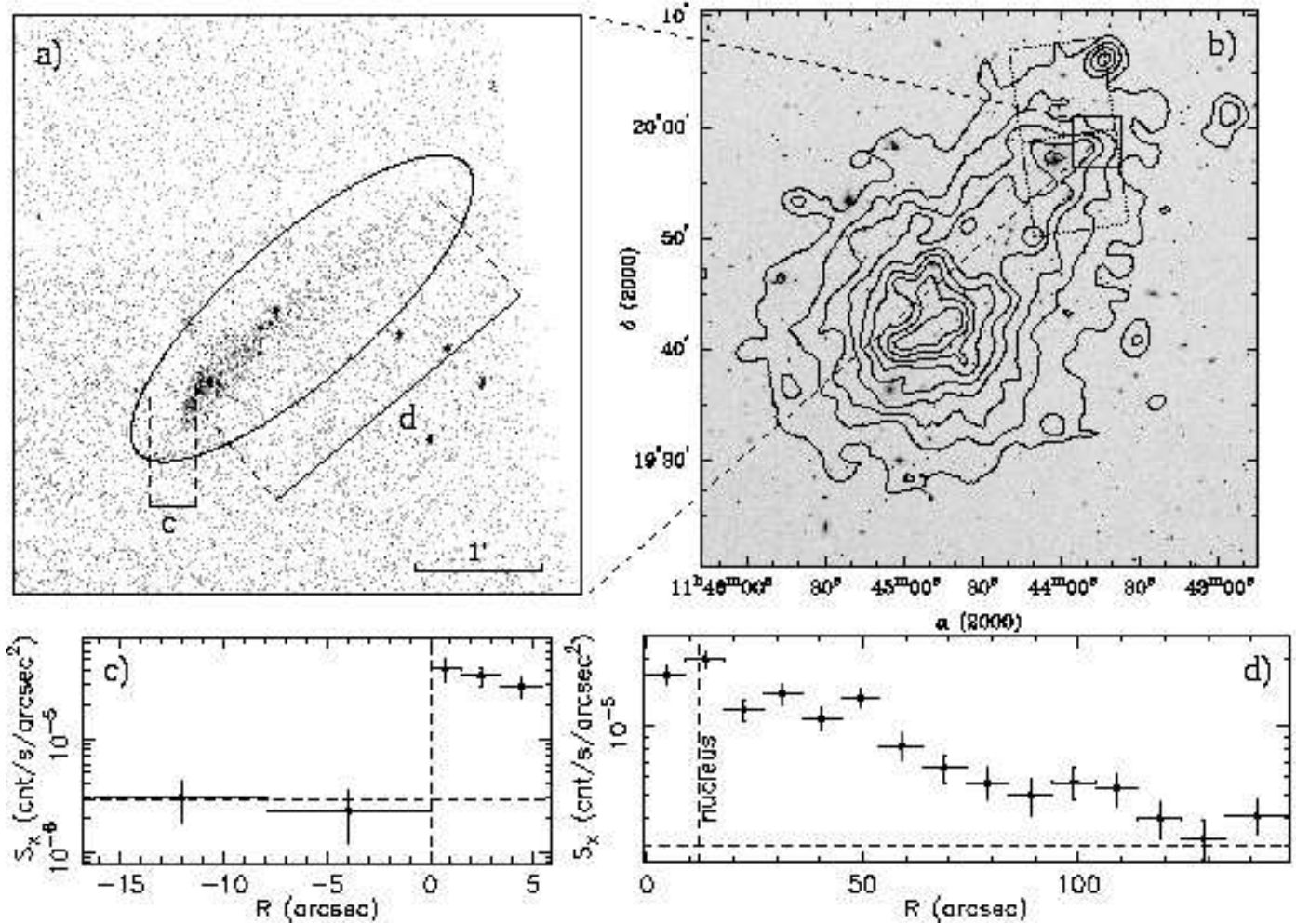


FIG. 1.— a): 0.5 - 2 keV *Chandra* count image of UGC 6697. A sharp surface brightness edge at the southeast end and a long tail to the northwest are significant. The detected X-ray emission is confined to the galactic plane. The selected contrast of the image does not show the point sources well, but four X-ray point sources are detected in UGC 6697 (shown in Fig. 2). The surface brightness is measured along the two narrow slices (shown in c and d). The ellipse is the region where the global spectrum of UGC 6697 diffuse emission was extracted (see §2.2). b): *ROSAT* contours of A1367 superposed on the DSS image. The two squares (dotted lines) show the S2 (north) and S3 (south) CCD fields. The small rectangle (solid lines) is the enlarged region (on the left). UGC 6697 is in a subcluster that is merging with the southeast subcluster. c): The surface brightness profile across the edge at the south end. Vertical box regions (8.36'' width) are used to measure the surface brightness. A brightness jump of  $\sim 13$  times is observed across the edge. The horizontal dashed line represents the background level (also in d). The width of the edge is less than 1.5'' or 0.7 kpc. d): The surface brightness profile (excluding point sources) along the galactic plane of UGC 6697 (20'' width adopted). The tail extends to the edge of the S3 chip.

TABLE 2  
THE X-RAY POINT SOURCES IN UGC 6697

	RA (2000)	decl. (2000)	counts (0.7 - 5 keV)	hardness ratio (1.4 - 5 keV / 0.7 - 1.4 keV)	note
P1	11:43:49.53	19:57:49.8	43 $\pm$ 7	1.02 $\pm$ 0.37	in a star cluster?
P2	11:43:49.46	19:58:03.1	55 $\pm$ 10	1.21 $\pm$ 0.36	
P3	11:43:49.12	19:58:07.3	110 $\pm$ 11	1.16 $\pm$ 0.28	UGC 6697 nucleus
P4	11:43:46.86	19:58:40.2	98 $\pm$ 10	0.80 $\pm$ 0.20	close to a star cluster?

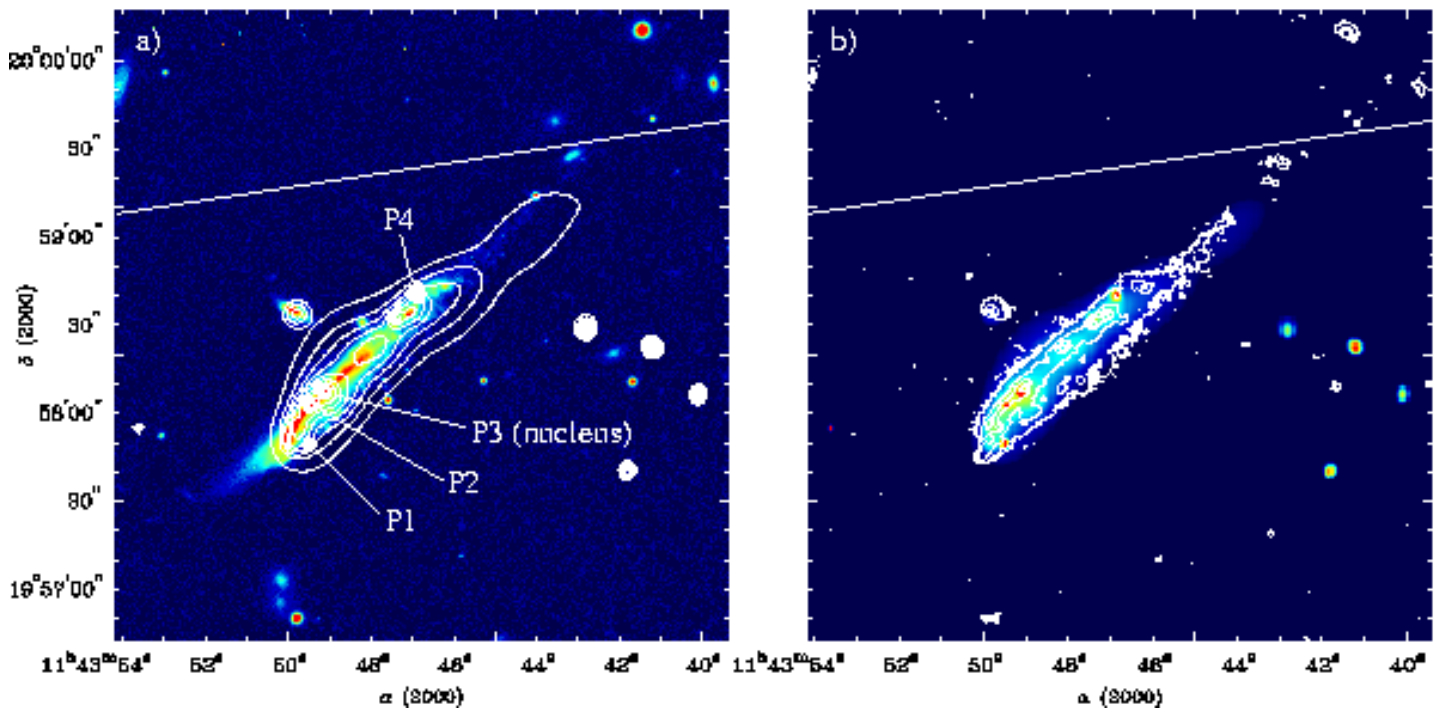


FIG. 2.— a): *Chandra* contours (from the exposure-corrected, and adaptively smoothed image by CSMOOTH) superposed on the B-band image of UGC 6697. Four X-ray point sources are marked. The contour levels increase by a factor of  $\sqrt{2}$  from the outermost one ( $10^{-3}$  counts/ksec/arcsec $^{-2}$ ). The solid white line is the S3 chip boundary (also in b). The X-ray sharp edge is well inside the optical light. The X-ray emission is more asymmetric than the optical light (P3 is the proposed nucleus), as the edge is only  $25''$  (or 11 kpc) from P3 but the tail extends to the edge of the S3 chip ( $140''$  or 61 kpc from P3, see Fig. 1). b): The H $\alpha$  contours of UGC 6697 superposed on the *Chandra* color image in the same field of a. The H $\alpha$  emission truncates at the same position where the X-ray sharp edge is located. A clumpy H $\alpha$  tail to the northwest, at the same position of the X-ray tail, is also observed. There is a general correlation between the H $\alpha$  emission and the diffuse X-ray emission.

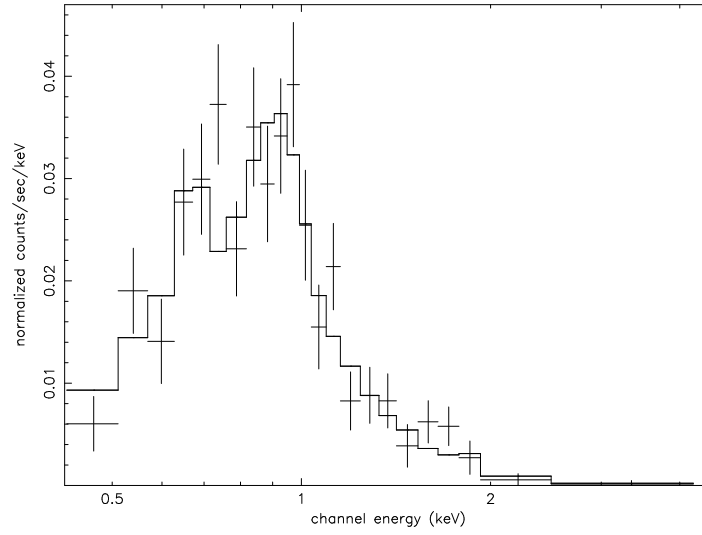


FIG. 3.— *Chandra* spectrum of the diffuse emission in UGC 6697 with the best-fit VMEKAL model. The blend of emission lines can be seen from 0.7 keV to 1 keV.

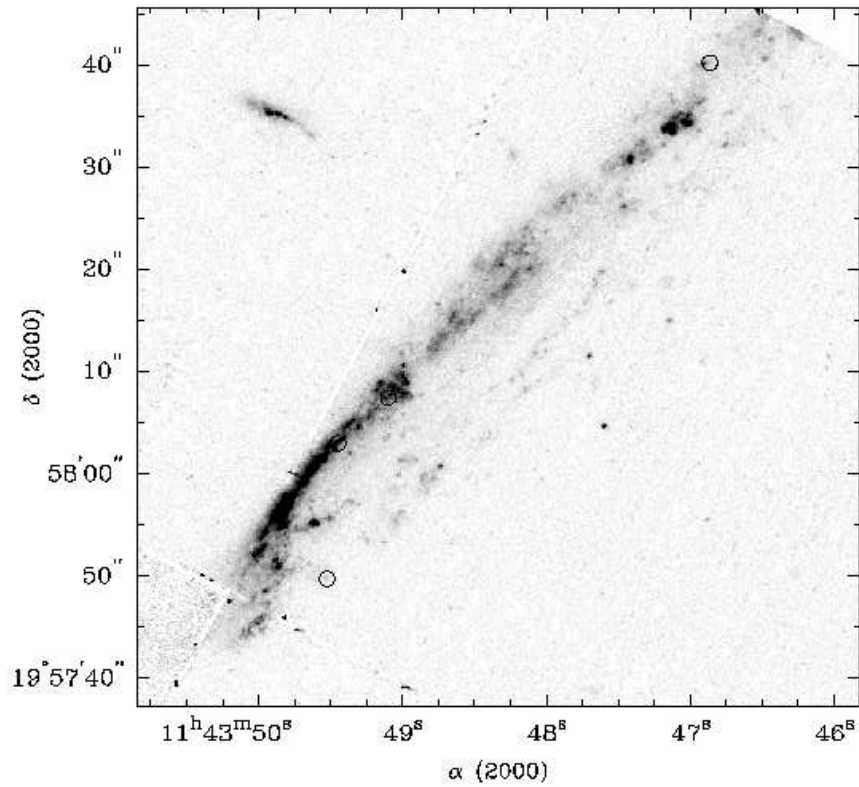


FIG. 4.— The positions of the four X-ray point sources superposed on the *HST* UV image (F300W filter) (P1 - P4, see Fig. 2). P3 is positionally coincident with the proposed nucleus of UGC 6697. P1 and P4 may be associated with star clusters.